

Fermi level density of states modulation without charge transfer in nickelate superlattices

Myung Joon Han ^{1,2,3} and Michel van Veenendaal ^{2,3}

¹ Department of Physics, Korea Advanced Institute of Science and Technology, Daejeon 305-701, Korea

² Advanced Photon Source, Argonne National Laboratory, Argonne, Illinois 60439, USA

³ Department of Physics, Northern Illinois University, De Kalb, Illinois 60115, USA

E-mail: mj.han@kaist.ac.kr

Abstract. By using first-principles density functional theory calculations for $(\text{LaNiO}_3)_m/(\text{SrTiO}_3)_n$ superlattices, we report a systematic way of electronic response to the interface geometry. It is found that Fermi level density of states of metallic nickelate layers is significantly reduced without charge transfer in the vicinity of interface to the insulating SrTiO_3 . This type of electronic state redistribution is clearly distinctive from other interface phenomena such as charge and orbital reconstruction. Our result sheds new light towards understanding the nickelates and other transition-metal oxide heterostructures.

PACS numbers: 73.20.-r, 71.20.-b

1. Introduction

Recent advances in the layer-by-layer growth technique of transition-metal oxide (TMO) heterostructures have created considerable research interest [1, 2]. In these artificially structured interfaces, many exotic material characteristics have been reported that are strikingly different from the bulk properties and the characteristics of a typical semiconducting interface (non-TMO interface) [1, 2]. For example, early studies of Ti-based superlattices such as $\text{LaTiO}_3/\text{SrTiO}_3$ (LTO/STO) and $\text{SrTiO}_3/\text{LaAlO}_3$ (STO/LAO) have revealed that heterostructuring induces unique electronic processes in TMOs that can dramatically change the macroscopic material properties [3, 4, 5, 6]. In these cases, it is widely believed that the valence charge reconstruction and the polar discontinuity can drive the interfaces to be metallic even if the two mother materials are good insulators. The orbital degrees of freedom are also found to be reconstructed at the interface between manganite and cuprate [7]. Other examples of emergent material properties caused by the heterostructure geometry include superconductivity [8] and magnetism [9, 10, 11]. These new findings raise the important question how the heterostructuring of TMO materials affects the density of states (DOS) close to the Fermi level and the related low-energy properties.

In this study, we report another type of electronic response to the interface geometry, that is, Fermi level DOS modulation caused by the state redistribution without valence change. Although this phenomenon exhibits similarities to the charge and orbital reconstruction, it displays distinctive characteristics. We found that the Fermi level DOS strongly modulates as a function of the location of nickel atoms relative to the interface. Our first-principles calculations of LaNiO_3 (LNO)/STO clearly demonstrate that this novel electronic modulation around the Fermi level is intrinsic to the structure itself, *i.e.*, the heterostructuring of nickelates, and not originating due to the other effects such as the charge transfer, oxidation, and valence change. Further analysis indicates that this kind of behavior can be a common feature of the nickelate system sandwiched by *any* wide-gap material. Our result sheds new light on the understanding of TMO interface phenomena.

It should be noted that $(\text{LNO})_m/(\text{STO})_n$ is distinctive from the widely-studied systems such as LNO/LAO and LNO film [12, 13, 14, 15, 16, 17, 18, 19] due to the possibility that Ti can have active d electrons around the Fermi level. The charge transfer can in principle take place between Ti and Ni. As an example, it would be instructive to compare LNO/STO to LNO/LTO superlattice in which the Ti can clearly have an electron in its d orbitals, and there may be the electron transfer from Ti to Ni, leading to the configuration of Ti as $d^{0+\delta}$ (or $d^{1-\delta}$ depending on the amount of charge transfer) and Ni as $d^{8-\delta}$ (or $d^{7+\delta}$) [20]. This kind of charge transfer is known to play an important role in determining the magnetic property of LNO/ LaMnO_3 (LMO) [21, 22, 23, 24]. However, in the case of LNO/STO, it is not clear if such an electron transfer would take place especially for the case of $m=n=1$. Note that $(\text{LNO})_1/(\text{STO})_1$ can also be identified as $(\text{SrNiO}_3)_1/(\text{LTO})_1$, and this alternative specification of the

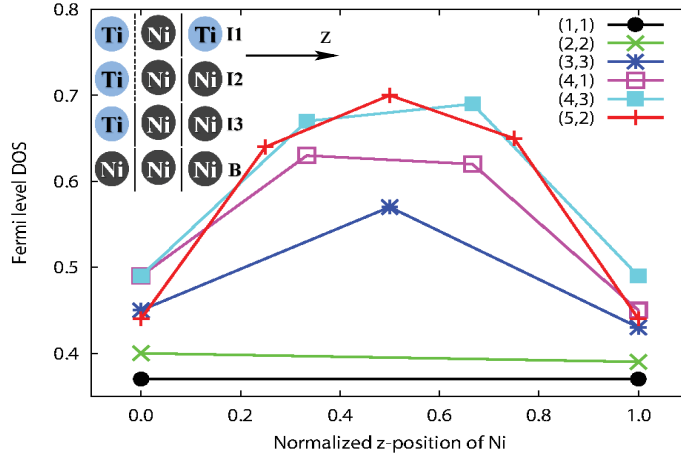


Figure 1. The calculated Fermi level DOS for various (m, n) combinations of superlattices. The z -axis positions of Ni ions are renormalized so that the first NiO_2 layer is located at $z = 0$ and the last is located at $z = 1$. (Inset) Four different types of Ni sites existing in the $(\text{LNO})_m/(\text{STO})_n$ superlattice. Dark gray and light blue circles represent Ni and Ti, respectively. Solid and dotted vertical bars in between transition metals represent SrO and LaO layers, respectively. Nickel of type I1 is located in between the TiO_2 -SrO and LaO- TiO_2 layers, type I2 in between TiO_2 -SrO and LaO- NiO_2 , and type I3 in between NiO_2 -LaO and LaO- TiO_2 . Nickel of type B is in the bulk-like arrangement located in between NiO_2 -LaO and LaO- NiO_2 .

system implies that Ti has d^1 (LTO-like) configuration instead of d^0 (STO-like). As we will show in the below, this possibility is not realized and Ti remains as d^0 even in the $m=n=1$ case, and Ni as d^7 (we drop off the indication of ligand hole for simplicity). From this interesting finding, important questions arise: If there is no charge transfer between the transition metal (TM) ions, what happens at the interface? In other words, under the condition that no charge transfer is allowed, what kind of response can be made by the metallic material, LNO, in the vicinity of interface to the insulating STO? The interface Ni would exhibit the same characteristics with the inner layer Ni? If not, what kind of possibility does Ni have in this superlattice geometry? This is a well defined open question that has never been addressed clearly before.

Our calculations show that the Ni- d states are actually adjusted at the interface in a systematic way that its DOS is redistributed while keeping the same total number of electrons. That is, the interface Ni, closer to the insulating STO, becomes more insulator-like in the sense that its Fermi level DOS gets reduced while the inner layer Ni more metal-like in the sense that the more DOS at the Fermi energy.

2. Computation Details

For band structure calculations, we employed the norm-conserving pseudopotential with a partial core correction, and a linear combination of localized pseudo-atomic orbitals (LCPAO) as a basis set [25]. We adopted the local density approximation (LDA) for the

exchange-correlation energy functional as parametrized by Perdew and Zunger [26], and used an energy cutoff of 400 Ry and k-grid of $12 \times 12 \times 6$ per unit volume. It is noted that bulk LNO is a paramagnetic metal down to low temperatures and that there is no report yet on the magnetic order in LNO/STO even if a theoretical calculation discussed the other possibilities [27]. Importantly, a recent standing-wave x-ray photoemission spectroscopy (SWXPS) measurement also assumed the paramagnetic phase [28], which will serve as a main experimental reference for our calculation. Therefore, a conventional LDA can be the best choice not only because it has been widely used in the previous studies to describe the paramagnetic LNO, but also because the LDA+U type of calculation has to assume a long-range ordered magnetic phase.

We used the Mulliken method for the charge analysis in which the Kohn-Sham states are projected onto our LCPAO basis orbitals. The number of Ni- e_g electrons obtained in this study is in the range comparable to the case of LNO/LXO (X: B, Al, Ga, In) superlattice systems as reported in Ref. 21. The geometry relaxation has been performed with the force criterion of 10^{-3} Hartree/Bohr. During the relaxation process, we assume that the in-plane lattice constant does not change due to its pinning with the substrate (we assumed the STO lattice parameter for the substrate).

3. Result

3.1. Classification of Ni types and modulation of Fermi level DOS

In LNO/STO, four different Ni sites exist considering their local environment. Nickel can be located either in between two $\text{La}^{3+}\text{O}^{2-}$ layers or in between the $\text{La}^{3+}\text{O}^{2-}$ and $\text{Sr}^{2+}\text{O}^{2-}$ layers. Further, its neighboring TM can be either titanium or nickel (see the inset of Fig. 1). If a nickel ion is located in between two $\text{La}^{3+}\text{O}^{2-}$ layers and its two neighboring TM sites are both Ni, it is bulk-like. At the interface, there are three different local structures denoted as I1, I2, and I3 in the inset of Fig. 1. As the electronic structure of Ni can be affected by both of these two factors (the neighboring TM ions and the ionic potentials caused by A-site cations), it is important to understand these effects on the Ni electronic structures. We will discuss this point below in further detail.

Recent depth-resolved SWXPS studies [28] show that the near-Fermi-level nickel states in $(\text{LNO})_4/(\text{STO})_3$ are significantly suppressed at the interface. A detailed analysis of the angular behavior of the SWXPS spectra indicates the electronic states reduction at the two outer LNO layers adjacent to the STO layers (type I2 and I3 nickel in our definition), but not in the inner layers (bulk-like nickel). It was speculated in Ref. 28 that the variation in Fermi level DOS could be due to the different oxidation of Ni ions; however, no further experimental evidence or explanation was provided.

3.2. DOS redistribution without charge transfer

We note that a clear understanding of this DOS modulation is of significant importance. If there is a charge transfer between TM ions, it is quite natural to expect that the

amount of DOS changes at the Fermi level. Interestingly, however, our calculation shows that such a charge transfer and oxidation process are not responsible for this DOS modulation. We performed calculations for $(\text{LNO})_m/(\text{STO})_n$ with $(m, n) = (1, 1), (2, 2), (3, 3), (4, 1), (4, 3)$, and $(5, 2)$, and found that the number of e_g electrons is 2.36–2.39 regardless of the type of nickel. From the point of view that all the nickels remain in the same charge status, the observed DOS modulation is unexpected and hard to be explained by the ‘electronic reconstruction’ processes that were suggested before.

The fact that there is no valence change or further oxidation of Ni may be most dramatically seen in $m=n=1$ case for which the alternative characterization of the superlattice as $(\text{SNO})_1/(\text{LTO})_1$ is also possible if the charge transfer (from Ni to Ti) might really happen. Since Ti has d^1 configuration in LTO while d^0 in STO, the result can be clearly seen in the Ti states. The calculated Ti- d DOS in Fig. 2(b) shows that all the Ti- d states are empty. Therefore one can identify the system as $(\text{LNO})_1/(\text{STO})_1$, and there is no charge transfer between Ni and Ti even in the $m=n=1$ case.

The effect of A -site cation potential asymmetry (*i.e.*, Sr^{2+} versus La^{3+}) does not cause any significant change in the electronic structure. This effect can be studied by examining the (3,3) heterostructure, for example, that contains both type I2 and I3 nickel ions (compare the dotted-blue with dashed-green line in Fig. 3(b)). Since the two nickel ions only differ due to the A -site cations, the different electronic structure reflects the effect due to the A -site asymmetry. Figure 3(b) shows that the DOS change is small. In addition, for other (m, n) structures, the projected DOS for type I2 and I3 nickel is always similar (seen in Fig. 4(b) for the case of (5,2) or upon comparison of Fermi level DOS value at $z = 0$ and $z = 1$ in Fig. 1). Therefore, the valence reconstruction is not relevant to this nickelate system presumably due to the strong covalency.

Now, considering that the nickel valence states are all same regardless of its position and the cation potential effect, it is quite surprising that the Fermi level DOS significantly varies. The calculated value of this quantity is summarized in Fig. 1 where the DOS values at the Fermi level (projected onto the different nickel sites) are plotted. It is clear that the interfacial nickel ions (see Fig. 1 where the z -position is normalized so that types I1, I2, and I3 located either at $z = 0$ or at $z = 1$) always have notably smaller Fermi level DOS than the bulk-like nickel ($0 < z < 1$ in Fig. 1). The difference becomes even more pronounced as the number of Ni layers increases from $m = 3$ to $m = 5$. For $m = 5$, the Fermi level DOS for the inner most layer Ni ions is larger by a factor ~ 2 when compared with that of the interfacial one. Since there is no charge transfer and no valence change, but a strong DOS modulation at the Fermi level, DOS should be redistributed in such a way that the total number of electrons is kept same. The further analysis shows that DOS is actually redistributed in a systematic way so that the Fermi level DOS gradually decreases as the nickelate layer gets closer to the interface. In order to make the charge valence unchanged, this weight is transferred to the lower energy part as schematically shown in Fig. 4(a). It is interesting to note that the metallic LNO layers become more insulator-like when they come closer to the insulating STO, while keeping the same valence charge; *i.e.*, the smaller number of states at the Fermi level.

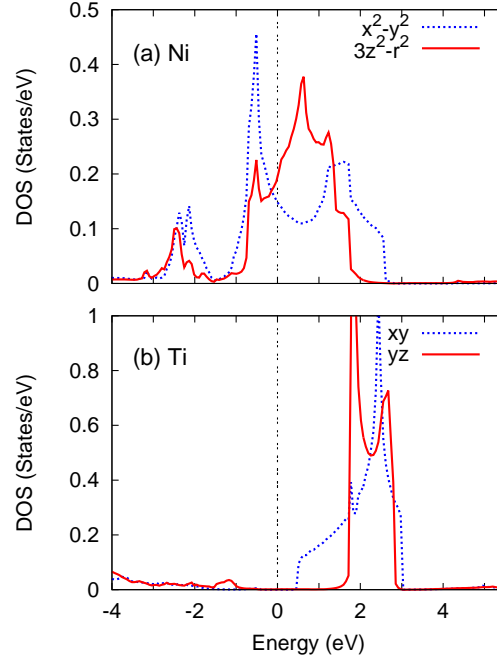


Figure 2. (a) Projected Ni- e_g DOS in the (1,1) superlattice. Red (solid) and blue (dashed) lines represent the $d_{3z^2-r^2}$ and $d_{x^2-y^2}$ states, respectively. (b) Projected Ti- t_{2g} DOS in the (1,1) superlattice. Blue-dashed and red-solid lines represent the d_{xy} and $d_{yz, zx}$ states, respectively. Vertical dotted lines indicate the position of Fermi energy.

On the other hand, the inner LNO layers far away from STO, become more metallic in the sense that they have more DOS at the Fermi level.

Fig. 4(b) shows that the reduction of DOS is quite significant. As seen in Fig. 4(b), the $d_{3z^2-r^2}$ states of the inner most (B; bulk-like) nickel is much larger than the two interface nickels (I2 and I3). The arrow indicates the DOS reduction at the Fermi level. The reduced states are transferred to the lower energy parts in case of interface nickel sites as clearly shown in the integrated DOS plot (Fig. 4(c)).

3.3. Mechanism of redistribution

To understand the mechanism behind the DOS modulation or redistribution process, a relatively simple picture can be considered based on the interactions between the molecule-like quantum states formed by the heterostructure geometry. As a starting point, let us consider the $m=n=1$ case. As seen in Fig. 2(a), the bandwidth of $d_{3z^2-r^2}$ state is markedly narrower than that of the $d_{x^2-y^2}$ state, which is a result of the limited hybridization along the z direction by the presence of STO layers. From this characteristics of $d_{3z^2-r^2}$ state, one can treat it as remnants of the molecular orbital character arising from a chain of m $d_{3z^2-r^2}$ orbitals along the z direction. These molecular-orbital-like features are further confirmed by the DOS shape of the (3,3) case; Figure 3(b) clearly shows the features related to the bonding, antibonding, and

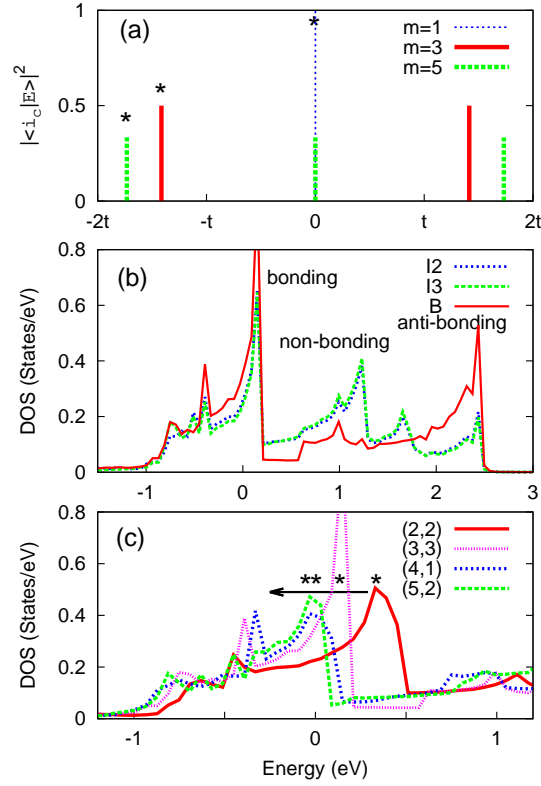


Figure 3. (a) Tight-binding calculation results for the weight of the central atom $|\langle i_c | E \rangle|^2$ in the energy eigenfunctions $|E\rangle$. The length of the chain corresponds to the thickness of the LNO layer, *i.e.*, m in $(\text{LNO})_m/(\text{STO})_n$. The central position is given by $i_c = m/2$ and $(m+1)/2$ for even and odd m , respectively. Energy unit is in the hopping parameter t . (b) Projected $d_{3z^2-r^2}$ DOS for (3,3) case. As expected, the bonding, non-bonding, and anti-bonding characteristics are most clearly seen in the case of (3,3). Type I2, I3, and B states are represented by blue-dotted, green-dashed, and red-solid lines, respectively. The Fermi level is set to be zero. (c) The projected $d_{3z^2-r^2}$ DOS for bulk-type Ni in the (3,3), (4,1), and (5,2) structures. For comparison, type I2 in (2,2) is also shown (red). The Fermi level is set to be zero. The asterisk marks indicate the peak positions.

nonbonding states of the $m = 3$ chain. It is noted that the DOS of the bulk-type nickel (solid-red line) is strongest in the bonding and antibonding features at ~ 0 and ~ 2.2 eV.

This point is further supported by our tight-binding analysis, which captures the essence of the features found in the first-principles results. Assuming that the system can approximately be treated as a linear chain of m -molecular orbitals, we constructed a tight-binding model Hamiltonian corresponding to N atoms, $H = \sum_{i=1}^N t c_i^\dagger c_j$, where c_i^\dagger creates an electron at the i th site in the z direction. The weight of the central (bulk-like) atom $|\langle i_c | E \rangle|^2$ is plotted in Fig. 3(a) as a function of energy E (in the unit of t). As the chain length, m , increases from $m = 1$ to 3 and 5, the states interact with each other and spread out over a wide energy range. For $m = 3$, the two-peak feature of bonding and anti-bonding is most clearly seen, which is consistent with the results of our first-principles calculation in Fig. 3(b). Another important point

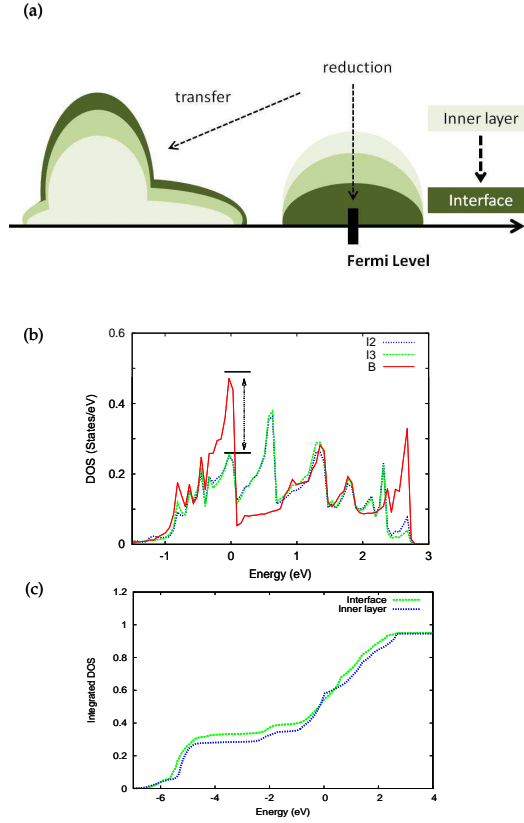


Figure 4. (a) Schematic illustration of DOS reduction at the Fermi level as a function of layer position relative to the interface. The reduced DOS is transferred to the lower energy part. (b) Projected $d_{3z^2-r^2}$ DOS of two interface layer nickels (blue and green) and the inner layer nickel (red) in the (5,2) superlattice. The arrow indicates the amount of DOS reduction. (c) The integrated $d_{3z^2-r^2}$ DOS for (5,2) case. The interface and inner-most layer state are depicted by green and blue color, respectively.

in this analysis is that the bonding-peak position gradually shifts toward the lower energy region as m increases (marked by the asterisks in Fig. 3(a)). Figure 3(c) shows that this characteristic behavior of the lower energy part of the $d_{3z^2-r^2}$ states is also found in the first-principles calculations: As the number of layers increases, the peak position (marked by asterisks in Fig. 3(c)) shifts towards the lower energy region. It is the electronic origin that leads to a strong modulation in the number of states at the chemical potential shown in Fig. 1.

4. Discussion

The Fermi level DOS modulation has distinctive features from the other interface reconstructions. In general, electronic [4] and orbital [7] reconstructions depend on the relative on-site energies of interfacial ions leading to a redistribution of charge between different sites and orbitals. In contrast, Fermi-level DOS modulations involve a strong

redistribution of states within the same sites and the same orbitals due to the presence of the interface. Since the low-energy properties are mainly determined by the states close to the chemical potential, strong position-dependent electronic properties can be expected and macroscopic properties (*e.g.*, resistivity) should be sensitive to these strong modulations. The direct observation of this kind of electronic response is difficult as the charge valence of the interface remains unchanged, and only the near-Fermi-level DOS should be measured. However, we note that SWXPS can be used for the verification of our results and that the recent experiment by Kaiser *et al.* for ($m=4$, $n=3$) compares well with our conclusion [28].

Our analysis can be applied to other superlattice structures with LNO sandwiched by *any* wide-gap insulator in which the hybridization is strongly blocked only along the z direction. Therefore, the same type of DOS modulation should be found in the related heterostructures unless the other types of response occur beforehand. To verify this point, we calculated the Fermi level DOS for $(\text{LNO})_m/(\text{LAO})_n$ with $(m, n) = (3, 3), (4, 1), (5, 2)$, and found that the same modulations occur in this different systems. It is noteworthy that our tight-binding analysis based on the molecular-orbital chain model is better applied to the case of LNO/LAO. The DOS modulation can be a universal feature in nickelate superlattices and possibly also in other interfaces in between metals and insulators.

Fermi level DOS reduction at the interfaces can provide an interesting new picture for the nickelate superlattices. We note that the DOS reduction at the interface is observed for all compositions of ($m \geq 3$, n), while for $m \leq 2$, only the interface nickel ions exist and there is no bulk-like one. Interestingly, several experiments on the nickelate superlattices independently report that the MIT occurs at $m \approx 3$. The same critical thickness was commonly observed in LNO/STO [30], LNO/LAO [31], LNO/SrMnO₃ [32], and LNO/LMO [22]. It is therefore tempting to relate the metallic and insulating phase to the bulk-like (B) and interface-like (I1, I2, I3) nickel layers, respectively, as the bulk-like nickel has more states at the Fermi energy and it start to appear at $m = 3$. Further, a recent experiment by Boris and co-workers reported that this MIT is accompanied with the paramagnetic to magnetic transition [31]. We note that, in the Kondo-type screening, the screening strength is governed by the Fermi level DOS as is clear from the Kondo temperature scale, $T_K \sim e^{-1/\rho_0 J_K}$, where ρ_0 refers to the Fermi level DOS. Therefore, it may be interesting to regard the nickelate superlattices as a kind of Kondo lattice system where the enhanced Fermi level DOS is responsible for the metallic conduction and simultaneously for the screening of local magnetic moments.

In the real experimental situations, there may be other possibilities for the nickelate layers to be adjusted in the heterostructure geometry. For example, the distortion of the oxygen octahedra and charge disproportionation can be important in the thin film LNO [33, 16, 27]. In this system of LNO/STO, a similar type of ionic displacement can also be realized [34, 27] although this possibility cannot be examined within our unitcell setup. Our calculations show that even without atomic distortion and/or charge transfer, the system has an electronic way of response to the interface geometry.

Since LDA has a limitation to describe electron correlations, the effect of correlation in Ni-3d on the DOS modulation can be an issue for the future study. Here we note the previous dynamical mean-field study for LNO/LAO-type of superlattice [17], which indicates that the electronic DOS is not much affected by increasing U as far as the double-counting energy is properly dealt with. Also considering the good agreement with SWXPS result, our conclusion is well justified at least for the paramagnetic and metallic region of phase space.

5. Summary

We report the Fermi level DOS modulation across the LNO layers in LNO/STO superlattices. This modulation is caused by the heterostructuring itself with no valence change or oxidation and in good agreement with a recent SWXPS experiment. It is related to but clearly distinctive from other interface phenomena such as orbital and valence reconstruction. Our analysis demonstrates that this electronic response to the hetero-interface structure originates from the novel process of quantum state formation and interactions between them. It can be related to MIT in the related systems, providing a new theoretical aspect to the complex-TMO research.

6. Acknowledgments

This work was supported by the U.S. Department of Energy (DOE), DE-FG02-03ER46097, and NIU's Institute for Nanoscience, Engineering, and Technology. The work at the Argonne National Laboratory was supported by the U.S. DOE, Office of Science, Office of Basic Energy Sciences under Contract No. DE-AC02-06CH11357. Computational resources were provided by the National Institute of Supercomputing and Networking/Korea Institute of Science and Technology Information with supercomputing resources including technical support (Grant No. KSC-2013-C2-005).

References

- [1] Mannhart J, Blank D H A, Hwang H Y, Millis A J and Triscone J M 2008 *Bulletin of the Materials Research Society* **33** 1027
- [2] Hwang H Y, Iwasa Y, Kawasaki M, Keimer B, Nagaosa N and Tokura Y 2012 *Nature Mater.* **11** 103
- [3] Ohtomo A, Muller D A, Grazul J L and Hwang H Y 2002 *Nature* **419** 378
- [4] Okamoto S and Millis A J 2004 *Nature* **428** 630
- [5] Ohtomo A and Hwang H Y 2004 *Nature* **427** 423
- [6] Nakagawa N, Hwang H Y and Muller D A 2006 *Nature Materials* **5** 204
- [7] Chakhalian J, Freeland J W, Habermeier H -U, Cristiani G, Khaliullin G, van Veenendaal M and Keimer B 2007 *Science* **318** 1114
- [8] Reyren N, Thiel S, Caviglia A D, Kourkoutis L F, Hammerl G, Richter C, Schneider C W, Kopp T, Rüetschi A -S, Jaccard D, Gabay M, Muller D A, Triscone J -M and Mannhart J 2007 *Science* **317** 1196

- [9] Brinkman A, Huijben M, van Zalk M, Huijben J, Zeitler U, Maan J C, van der Wiel W G, Rijnders G, Blank D H A and Hilgenkamp H 2007 *Nature Mater.* **6** 493
- [10] Li L, Richter C, Mannhart J and Ashoori R C 2011 *Nature Phys.* **7** 762
- [11] Bert J A, Kalisky B, Bell C, Kim M, Hikita Y, Hwang H Y and Moler K A 2011 *Nature Phys.* **7** 767
- [12] Son J, Moetakef P, LeBeau J M, Ouellette D, Balents L, Allen S J and Stemmer S 2010 *Appl. Phys. Lett.* **96** 062114
- [13] Hansmann P, Toschi A, Yang X, Andersen O K and Held K 2010 *Phys. Rev. B* **82** 235123
- [14] Han M J, Marianetti C A and Millis A J 2010 *Phys. Rev. B.* **82** 134408
- [15] Han M J and van Veenendaal M 2011 *Phys. Rev. B* **84** 125137
- [16] Liu J, Okamoto S, van Veenendaal M, Kareev M, Gray B, Ryan P, Freeland J W and Chakhalian J 2011 *Phys. Rev. B* **83** 161102(R)
- [17] Han M J, Wang X, Marianetti C A and Millis A J 2011 *Phys. Rev. Lett.* **107** 206804
- [18] Han M J and van Veenendaal M 2012 *Phys. Rev. B* **85** 195102
- [19] Sakai E, Tamamitsu M, Yoshimatsu K, Okamoto S, Horiba K, Oshima M and Kumigashira H 2013 *Phys. Rev. B* **87** 075132
- [20] Chen H, Marianetti C A and Millis A J 2013 *Phys. Rev. Lett.* **111** 116403
- [21] Gibert M, Zubko P, Scherwitsl R, Íñiguez J and Triscone J -M 2012 *Nature Mater.* **11** 195
- [22] Hoffman J, Tung I C, Nelson-Cheeseman B B, Liu M, Freeland J W and Bhattacharya A, 2013 *Phys. Rev. B* **88** 144411
- [23] Dong S and Dagotto E, 2013 *Phys. Rev. B* **87** 195116
- [24] Lee A T and Han M J 2013 *Phys. Rev. B* **88**, 035126
- [25] <http://openmx-square.org>.
- [26] Perdew J P and Zunger A 1981 *Phys. Rev. B* **23** 5048 Ceperley D M and Alder B J, 1980 *Phys. Rev. Lett.* **45** 566
- [27] Kim H -S and Han M J 2013 arXiv:1306.0713
- [28] Kaiser A M, Gray A X, Conti G, Son J, Greer A, Perona A, Rattanachata A, Saw A Y, Bostwick A, Yang S, Yang S -H, Gullikson E M, Kortright J B, Stemmer S and Fadley C S 2011 *Phys. Rev. Lett.* **107** 116402
- [29] Han M J, Marianetti C A and Millis A J 2010 *Phys. Rev. B.* **82** 134408
- [30] Son J, LeBeau J M, Allen S J and Stemmer S 2010 *Appl. Phys. Lett.* **97** 202109
- [31] Boris A V, Matiks Y, Benckiser E, Frano A, Popovich P, Hinkov V, Wochner P, Castro-Colin M, Detemple E, Malik V K, Bernhard C, Prokscha T, Suter A, Salman Z, Morenzoni E, Cristiani G, Habermeier H -U and Keimer B 2011 *Science* **332** 937
- [32] May S J, Santos T S and Bhattacharya A 2009 *Phys. Rev. B* **79** 115127
- [33] Chakhalian J, Rondinelli J M, Liu J, Gray B A, Kareev M, Moon E J, Prasai N, Cohn J L, Varela M, Tung I C, Bedzyk M J, Altendorf S G, Strigari F, Dabrowski B, Tjeng L H, Ryan P J and Freeland J W 2011 *Phys. Rev. Lett.* **107** 116805
- [34] Hwang J, Son J, Zhang J Y, Janotti A Van de Walle C G and Stemmer S 2013 *Phys. Rev. B* **87** 060101(R)